RESEARCH ARTICLE

Difunctional Adsorbents Ni/ZnO–HZSM-5 on Adsorption Desulfurization and Aromatization of Olefin Reaction

Jianzeng Du[1,2,3] · Yonghong Li[1,2,3] · Zhenyu Miao[1,2,3]

Abstract

Novel Ni/ZnO–HZSM-5 adsorbents were synthesized by incipient wetness impregnation. The Ni/ZnO–HZSM-5 adsorbent can achieve deep desulfurization and olefin aromatization at the same time. Thiophene sulfur was removed from 495 to less than 10 ppm via reactive adsorption desulfurization (RADS). Olefins were also converted into aromatics. HZSM-5 did not only support adsorbents but also cooperated with active Ni sites to catalyze olefins into aromatic hydrocarbons. Aromatization of 1-pentene, 2-pentene, 2-methyl-2-butene, and 1-hexene on adsorbents was investigated. The adsorbents were characterized by the Brunauer–Emmett–Teller, X-ray diffraction, temperature-programmed reduction, and temperature-programmed desorption of ammonia and thermogravimetric analysis. The experimental results showed that strong acids on the adsorbent disappeared after HZSM-5 loaded active metal sites, and almost no coke was generated on adsorbents in RADS.

Keywords Ni/ZnO-HZSM-5 · Desulfurization · Olefin aromatization

Introduction

Deep desulfurization of fossil fuels and upgrading the quality of gasoline will be an inevitable tendency for stringent environmental legislations in various countries. Fluid catalytic cracking (FCC) gasoline contains large amounts of olefins and thiophene sulfides [1]; besides, olefins are unstable. Therefore, if olefins can be efficiently converted to other high-octane and stable components such as aromatics or isoparaffins, the quality of gasoline will significantly improve, and the octane number of gasoline will also be maintained at the same time. Currently, the technology of deep desulfurization is very mature, especially reactive adsorption desulfurization (RADS). If RADS can couple olefin aromatization or isomerization together, the quality of FCC gasoline will improve, and the fuel refining industry will also save high amounts of energy.

The traditional adsorbent of RADS consists of Ni/ZnO–Al$_2$O$_3$–SiO$_2$; adsorbents have also performed superiorly in deep desulfurization of FCC gasoline [2–4]. The active component Ni plays a key role in adsorbing sulfur atoms [5]. Organic sulfide compounds are first adsorbed by Ni atoms, and Ni continuously removes the sulfur atoms from organic sulfides, generating NiS [6]. NiS would be reduced by H$_2$ and release H$_2$S. Finally, H$_2$S is captured rapidly by ZnO and produces ZnS based on chemical Eqs. (1), (2), and (3) [7]. The mechanism of adsorption has been put forward by Song [8] and Velu et al. [9], who considered that organic sulfide compounds were adsorbed on active metal Ni sites via direct sulfur–adsorbent (S–M) interaction, forming organometallic complexes, rather than by π-complexation. Wang et al. [10] also confirmed that thiophene was adsorbed via direct S–M interaction through the study of adsorption heat, whereas olefins were adsorbed through π-complexation. However, although S–M interactions are much stronger than π-complexation, they still exhibit fierce competitive adsorption due to the larger quantity of olefins than sulfides in FCC gasoline. As a result, this competitive adsorption would decrease the selectivity of desulfurization on the adsorbents, and olefins would saturate in the H$_2$ atmosphere. Therefore, studies attempt to find

✉ Yonghong Li
  yhli@tju.edu.cn

1   Key Lab for Green Chemical Technology of Ministry of Education, School of Chemical Engineering and Technology, Tianjin University, Tianjin 300350, China

2   National Engineering Research Center for Distillation Technology, Tianjin 300350, China

3   Collaborative Innovation Center of Chemical Science and Engineering, Tianjin 300350, China

methods to enhance the selectivity of adsorption and avoid olefin saturation. Khare [11, 12] put forward a formulation in which active sites consist of Ni and Co and expected that Ni and Co could play a synergistic role to enhance the ability of RADS. Wang et al. [13] demonstrated that Ni and Co are the best active metal sites by density functional theory. Skrzypski et al. [14] used Mo as auxiliaries to prepare adsorbents which could increase the specific surface area and pore volume. Ju et al. [15] used Ca to promote the dispersion of active Ni sites and enhance desulfurization and regeneration ability of adsorbents.

$$Ni + RSH = NiS + RH, \tag{1}$$

$$NiS + H_2 = Ni + H_2S \tag{2}$$

$$ZnO + H_2S = ZnS + H_2O \tag{3}$$

However, although the adsorbent Ni/ZnO–Al$_2$O$_3$–SiO$_2$ could realize deep desulfurization and control the concentration of sulfur under 10 mg/kg, a part of olefin would react through hydrogenation saturation [16–18], resulting in the loss of octane value. ZnO, Ni, and Al$_2$O$_3$ would easily combine together and generate irreversible spinel of ZnAl$_2$O$_4$ and inactive NiAl$_2$O$_4$ in Ni/ZnO–Al$_2$O$_3$–SiO$_2$ adsorbent [17]. Therefore, novel adsorbents must be developed for desulfurization and maintaining octane number. Porous materials, such as Al$_2$O$_3$ or SiO$_2$ and HZSM-5, could be used as matrix owing to their large specific surface area [19]. HZSM-5 possesses large specific surface area, unique micropore channels, and stable structural characteristics. Particularly, HZSM-5 can resist coking and olefin aromatization [20–22]. Accordingly, HZSM-5 is the ideal material for olefin aromatization and isomerization [23–25]. HZSM-5 loading Ni or Zn would increase the amount of Lewis acid sites and decrease Bronsted acid sites [26]. Lewis acid sites favor the olefin aromatization and isomerization [26].

We aim to convert olefins into aromatics and isoparaffin during RADS, achieving the deep desulfurization and maintaining the octane number at the same time. In this paper, HZSM-5 was used as carrier to load Ni–ZnO and to synthesize difunctional Ni/ZnO–HZSM-5 adsorbents for deep desulfurization and reduction of olefins. The adsorbents were evaluated with RADS using four different olefins as feedstock, and the samples were characterized with a series of techniques.

Experiment

Chemicals and Feedstock

The chemicals and feedstock included 1-hexene (Macklin, 99%), 1-pentene (TCI, 99.0%), 2-pentene (TCI, 99.0%, trans 95.0%), 2-methyl-2-butene (Aladdin, 99%), n-heptane (Aladdin, 98.5%), thiophene (TCI, 98.0%), Ni(NO$_3$)$_2$·6H$_2$O (Aladdin, 99.0%) and Zn(NO$_3$)$_2$·6H$_2$O (Aladdin, 99.0%), HZSM-5 (Nankai University Catalyst Co., Ltd, China), and γ-Al$_2$O$_3$ (Aladdin, 99.0%). The model hydrocarbon comprised 35.0 wt% olefin and 65.0 wt% n-heptane. Sulfur concentration reached 495 mg/kg and was represented by 1300 mg/kg thiophene in the model feedstock.

Adsorbent Preparation

Ni/ZnO–HZSM-5 adsorbents with different ratios of Ni/ZnO were synthesized by incipient wetness impregnation. HZSM-5 was calcinated at 500 °C for 3.0 h before using. A total of 4.95 g of Ni(NO$_3$)$_2$·6H$_2$O was dissolved in 6.0 mL distilled water and followed by the addition of 6.1 g of Zn(NO$_3$)$_2$·6H$_2$O under stirring at 90 °C in water bath. The mixture solution was dropwise added into 4.0 g HZSM-5 and ultrasound-treated for 15 min, followed by stirring at 90 °C in water bath for 4 h, evaporating the redundant water. The mixture was aged at 25 °C for 8 h. After aging, the mixture was dried at 120 °C overnight and followed by calcination at 550 °C in air for 6 h in a muffle furnace. The temperature of the muffle furnace was heated up to 550 °C with a ramp rate of 4 °C per min. Finally, the powder was tableted and ground to 20–40 mesh adsorbents. For comparison purposes, Ni/ZnO–Al$_2$O$_3$ adsorbent was synthesized using the same method, and Ni/ZnO was synthesized by co-precipitation. The adsorbents with different ratios of Ni/ZnO were numbered, as shown in Table 1.

Adsorbent Performance Evaluation and Analytic Procedure

RADS performance of adsorbents was evaluated in a fixed bed microreactor using thiophene as a model sulfur compound. A steel microreactor with an internal diameter of 6 mm and 600 mm in length was used for experiment. A total of 1.0 g (20–40 mesh) adsorbent was loaded into the constant-temperature zone of the microreactor column and embedded between glass wool plugs. Before RADS experiment, Ni/ZnO–HZSM-5 was first reduced for conversion of NiO into Ni in the presence of H$_2$ with a flow rate of 30 mL/min under 2.0 MPa and at 470 °C for 2 h. After reduction,

Table 1 Adsorbent numbers

No.	Adsorbent
1	Ni/ZnO-HZSM-5-1:1
2	Ni/ZnO-HZSM-5-1:1.5
3	Ni/ZnO-HZSM-5-1:2
4	Ni/ZnO–Al$_2$O$_3$
5	Ni/ZnO

the temperature of adsorbent bed was set to 400 °C, and the pressure was unchanged at 2.0 MPa. Then, the model fuel was preheated at 120 °C and then fed into the microreactor by liquid pump at a weight hourly space velocity of 4.1 h^{-1} and H$_2$/oil volume ratio of 100. The deactivated adsorbents were regenerated at 480 °C with an air flow rate of 30 mL/min under 0.5 MPa. Product composition was analyzed with gas chromatography–mass spectrometry (GC–MS) (Agilent 7890) and a Fuli 9790 gas chromatograph using a flame ionization detector. The total sulfur content in the liquid product was analyzed with a flame photometric detector (Fuli 9790). Adsorption capacity of thiophene sulfur was calculated by Eq. (4):

$$C = \left(C_0 V - C_1 V\right)/m \tag{4}$$

where C_0 refers to the initial sulfur concentration; V is fuel flow; C_1 is the sulfur concentration in RADS product; and m is weight of adsorbents.

Adsorbent Characterization

X-ray diffraction (XRD) measurements were taken on a Bruker D 8-Focus and advanced X-ray diffractometer (Cu Kα $\lambda = 0.15418$ nm, 40 kV, and 40 mA) in the step scanning mode with 2θ between 20° and 80° at a scanning step of 5°/min. The reducibility of adsorbents was investigated by hydrogen temperature-programmed reduction (H$_2$-TPR) technique using the apparatus of Xianquan TP-5079, and reduction temperature ranged from 60 to 770 °C with a ramp rate of 10 °C per min. N$_2$ sorption experiments of Ni/ZnO–HZSM-5 were performed at 77 K by a Micromeritics ASAP 2020 analyzer. Prior to the analysis, adsorbents were degassed at 300 °C for 6 h under N$_2$. The surface area was calculated from the adsorption branch in the range of relative pressure from 0.050 to 0.295 by Brunauer–Emmett–Teller (BET) method. The micropore volume was calculated by t-Polt method, and the pore size distribution (PSD) was derived from the adsorption branch of isotherms based on the Horvath–Kawazoe method. The profiles of temperature-programmed desorption of ammonia (NH$_3$-TPD) were carried out on a Xianquan TP-5076 TPD analyzer with a thermal conductivity detector (TCD). Finally, thermogravimetric analysis (TG) was performed in air flow (25 mL/min) on Shimadzu-TGA-50 apparatus. Temperature ranged from 35 to 750 °C with a heating rate of 10 °C per min.

Results and Discussion

RADS Performance of Adsorbents

Figure 1 presents the RADS performance and sulfur adsorption capacities (mg/g) of Ni/ZnO–HZSM-5-X adsorbents; the model fuel comprises 34.3% 1-hexene and 65.5% n-heptane. The Ni/ZnO–HZSM-5-1:1 adsorbent exhibited an excellent RADS performance with high thiophene conversion of 98.5% before the first 12 mL model fuel and gradually decreased to 95.6% with the model fuel of 20 mL. The corresponding cumulative sulfur adsorption capacity measured 7.34 mg/g. In the case of Ni/ZnO–HZSM-5-1:1.5 and Ni/ZnO–HZSM-5-1:2, sulfur adsorption capacity reached 7.21 and 6.87 mg/g, respectively. Thiophene conversion of Ni/ZnO–HZSM-5-1:1.5 remained above 98.0% before 12 mL. After 20 mL of model fuel, thiophene conversion reduced drastically. The order of desulfurization ability is as follows: Ni/ZnO–HZSM-5-1:1 > Ni/ZnO–HZSM-5-1:1.5 > Ni/ZnO–HZSM-5-1:2. The difference in RADS activity is mainly ascribed to the number of active Ni atoms distributed on the adsorption surface. The used Ni/ZnO–HZSM-5-1:1.5 adsorbents were regenerated, and Ni/ZnO–HZSM-5-1:1.5 (R) was applied again for RADS test. As shown in Fig. 1b, the RADS performance of Ni/ZnO–HZSM-5-1:1.5 (R) was as good as the fresh materials.
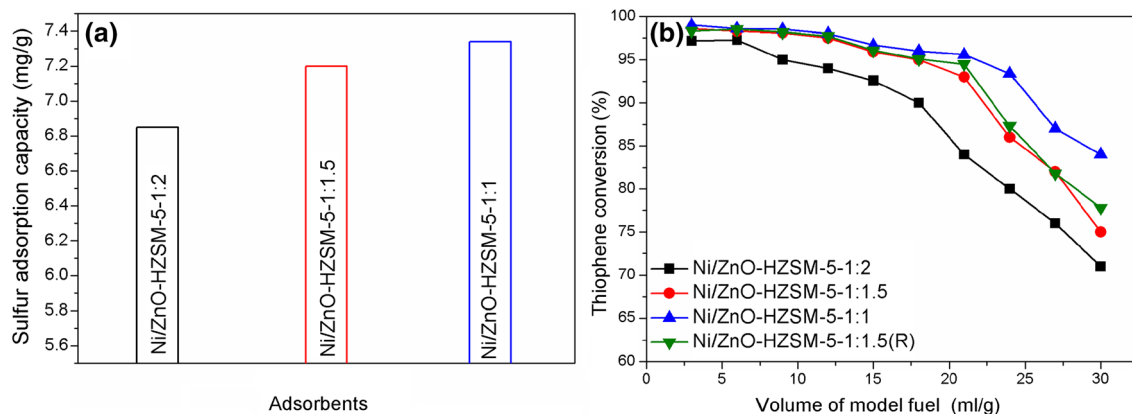

Fig. 1 **a** Sulfur adsorption capacity of adsorbents at 24 mL model fuel and **b** RADS profile of adsorbents

Olefin aromatization was also investigated. Aromatics yield of Ni/ZnO–HZSM-5-1:1, Ni/ZnO–HZSM-5-1:1.5, and Ni/ZnO–HZSM-5-1:2 reached 58.5, 67.1, and 63.7%, respectively. The conversion of olefins to aromatics showed a nonlinear correlation with the amount of Ni atoms. Studies have reported that ZnO could also enhance the catalysis of olefin aromatization [27]. Thus, ZnO would act synergistically with Ni in aromatization. Otherwise, aromatics yield of Ni/ZnO–HZSM-5-1:1 would not reach lower than that of Ni/ZnO–HZSM-5-1:2. The aromatics yield of Ni/ZnO–HZSM-5-1:1.5 was higher than those of Ni/ZnO–HZSM-5-1:2 orand Ni/ZnO–HZSM-5-1:1. Desulfurization performance of Ni/ZnO–HZSM-5-1:1.5 adsorbent was almost the same as that of Ni/ZnO–HZSM-5-1:1 before the 15 mL model fuel. Thus, in the following study, we focused on using the Ni/ZnO–HZSM-5-1:1.5 adsorbent to study the performance of desulfurization and aromatization. Unless special instructions were provided, the adsorbent considered was Ni/ZnO–HZSM-5-1:1.5.

Comparison of Thiophene Desulfurization and Aromatization in C_5 Olefins

To investigate the influences between aromatization and desulfurization, three kinds of C_5 isomeride olefins were tested on Ni/ZnO–HZSM-5-1:1.5. Table 2 presents the composition distributions of RADS product with different model fuels.

In comparison with the three olefins, 2-methyl-2-butene (35.2%) exhibited the best performance in desulfurization but also the poorest performance in aromatization. Model fuel volume was about 15 mL when the concentration of sulfur in 2-methyl-2-butene product reached 10 ppm, whereas model fuel volumes of 1-pentene (35.0%) and 2-pentene (35.4%) were 9 mL and 11 mL, respectively. The three converted olefins decreased in the order of 2-pentene > 2-methyl-2-butene > 1-pentene, as shown in Fig. 2a. However, aromatization reactivity of the three isomers is opposite to the olefin conversion reactivity, whose order is 1-pentene > 2-pentene > 2-methyl-2-butene, as shown in Fig. 2b. The results suggest that the positions of carbon–carbon double bonds and branched chains in the olefins would significantly affect their reactivity, but olefin aromatization reactivity showed no positive correlation with conversion reactivity. Although 2-pentene and 2-methyl-2-butene produced relatively less aromatics than 1-pentene, they produced relatively larger amounts of isoparaffins and cyclopentane, respectively, which are also superior high-octane supporter in gasoline.

Olefins are adsorbed on adsorbents via the π-complexation that connects the carbon atom with Ni [10].

Table 2 Product composition with different model fuels

Product	Product composition (wt%)		
	1-pentene (35.0%)	2-pentene (35.4%)	2-methyl-2-butene (35.2%)
2-Methylpropene	0.5	1.6	1.7
2-Methylbutane	4.6	4.8	5.3
Butane	–	–	0.6
Pentane	0.6	1.2	0.8
1-Pentene	7.5	–	–
2-Pentene	–	5.7	–
2-Methyl-2-butene	–	–	6.1
Cyclopentane	2.1	4.5	5.6
Benzene	1.3	1.0	0.9
n-Heptane	59.8	63.3	64.0
Toluene	12.6	8.3	7.4
Xylene	10.6	8.8	6.8
1-Ethyl-2-methylbenzene	0.4	0.6	0.5

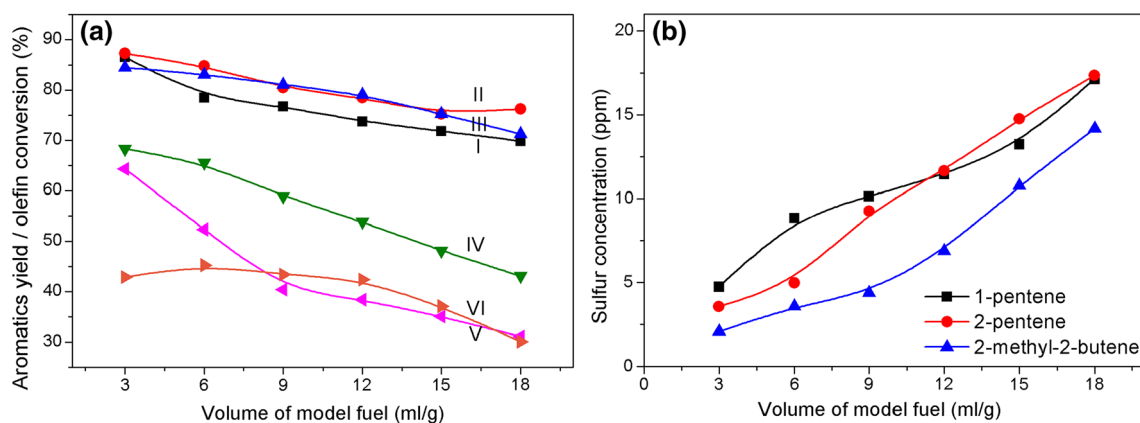**Fig. 2** **a** Olefin aromatics yield/olefin conversion (I, II, III: conversion; IV, V, VI: yield. I, IV: 1-pentene; II, V: 2-pentene; III, VI: 2-methyl-2-butene) and **b** RADS profiles of adsorbents using different model fuels as feedstock

π-Complexation would be enhanced if the carbon atoms with double bonds connect the electron-donating group, similar to methyl. Therefore, the adsorption ability of the three isomers decreased in the following order: 2-methyl-2-butene > 2-pentene > 1-pentene. The carbon atoms with double bonds connecting the electron-donating group would be more conducive to be adsorbed on adsorbents and thus would feature more opportunities to participate in reactions. On the other hand, in olefin aromatization, the first step of the reaction results in carbocation [28], in which olefins with branched chains show advantage for their thick electron density. However, the intermediate carbocation with branches is not conducive to oligomerization and cyclizing as positive charges are weakened by the electronic effect, which would decrease the yield of aromatics.

The heptane proportion in the product of 1-pentene decreased by 5.2%, while heptane in the product of 2-pentene or 2-methyl-2-butene remained almost unchanged. Notably, this result indicates that heptane in the 1-pentene model fuel participates in reactions. This finding is also ascribed to 1-pentene (the weakest among the three isomers) adsorption on the adsorbent. Thus, heptane possesses more opportunities to be adsorbed on the adsorbent and undergo chemical reaction. The product of pure heptane showed almost no contribution to aromatic hydrocarbon, as shown in Table 3.

Comparison of Thiophene Desulfurization and Aromatization Between 1-Pentene and 1-Hexene

Comparing 1-hexene (34.3%) with 1-pentene (35.0%), the conversion rate of 1-hexene (88.9%) was higher than that of 1-pentene (79.4%) at the reaction time of 1.0 h on the Ni/ZnO–HZSM-5-1:1.5, as shown in Table 4. The aromatics yield of 1-hexene was lower than that of 1-pentene, whereas 1-hexene exhibited better desulfurization performance than 1-pentene, as shown in Fig. 3. The results agree with the discussion in Section "Comparison of thiophene desulfurization and aromatization in C_5 olefins." In a word, under good olefin aromatization, thiophene desulfurization would be weakened. One of the reasons for the weaker aromatization of 1-hexene than 1-pentene is that the pore size of HZSM-5 was fixed and measured less than 0.45 nm (as shown in Fig. 7), and HZSM-5 featured very high selectivity. The fixed pore resulted in higher molecular volume, causing the more disadvantageous generation of aromatics [29]. This result also explains why the predominant aromatic

Table 4 Product composition of different adsorbent used model fuel: 1-hexene (34.3%) and n-heptane (65.5%)

Product	Product composition (wt%)	
	Ni/ZnO–HZSM-5-1:1.5	Ni/ZnO–Al$_2$O$_3$
2-Butene	–	0.7
Isobutane	1.8	–
Butane	3.5	–
2-Methyl-1-propene	–	0.6
2-Methylbutane	5.4	–
2-Pentene	–	1.1
Pentane	1.3	–
2-Methylpentane	2.3	–
2-Methyl-1-pentene	–	1.3
3-Methyl-2-pentene	–	1.7
3-Methylpentane	0.3	–
n-Hexane	0.4	1.4
4-Methyl-2-pentene	–	2.1
2,3-Dimethyl-2-butene	–	1.5
1-Hexene	3.8	20.4
Benzene	1.0	–
n-Heptane	57.6	68.8
2-Methyl-2-hexene	–	0.3
Toluene	12.2	–
Xylene	8.7	–
1-Ethyl-2-methylbenzene	1.3	–
2-Methylnaphthalene	0.3	–

hydrocarbons included toluene and xylene rather than the low-molecular-weight benzene or other higher aromatics. A low benzene yield enables the quality of product to meet the strict regulation on benzene content in clean gasoline. Based on the above analysis and olefin product analysis in Tables 2 and 4, C_5 olefins easily generated naphthene, whereas 1-hexene experienced difficulty in generating the same compound, resulting in almost no naphthene in the product. These findings imply that the reaction mechanism of olefin aromatization between C_5 and C_6 may be different.

Reaction Mechanism

The product distribution of Ni/ZnO–Al$_2$O$_3$ was analyzed by GC–MS, as shown in Table 4. The main products were 1-hexene isomerides with branched chains, accounting for 8.0%. The results imply that rearrangement reaction

Table 3 Product composition of 100% n-heptane (wt%)

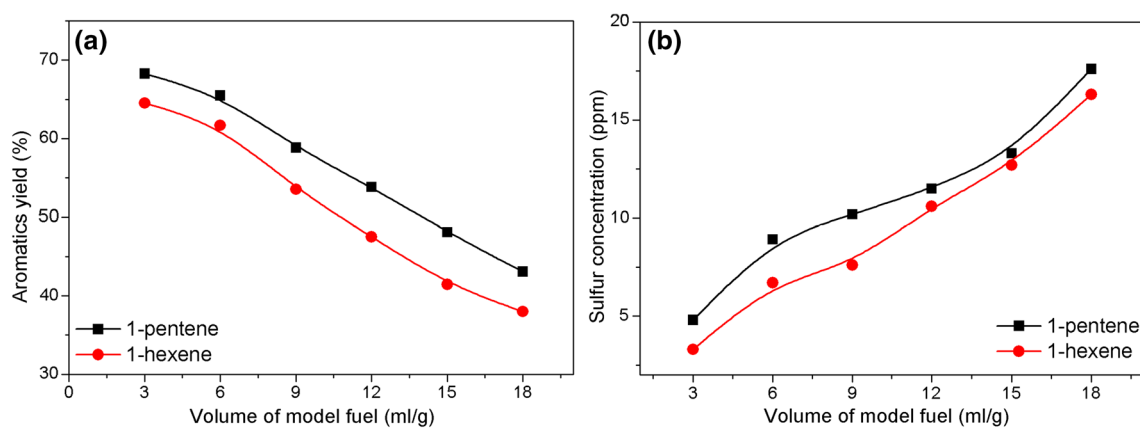| C4	Pentane	3-Methylhexane hexane	n-Heptane	Methyl-cyclohexane	Toluene	Xylene
1.7	1.2	0.6	92.9	0.8	1.3	1.5

C4: butane and 2-methyl-1-propene

Fig. 3 a Aromatics yield and **b** RADS profiles of adsorbents using 1-pentene and 1-hexene model fuel as feedstock

occurred on the active Ni sites. Based on the above discussion and experimental phenomena, we infer that the competition between sulfides and olefins did not only exist in physical adsorption on the adsorbent surface but also in subsequent chemical reaction on active Ni sites. In this process, hydrogen molecules reacted with Ni to produce H-positive and H-negative ions. Then, the H-positive ions attacked the 1-hexene adsorbed on Ni by π-bond formation to generate carbocation [30]. Next, the carbocation molecules underwent structural rearrangements and generated branched isomers on the Ni surface [31], which follows the minimum energy principle. However, while HZSM-5 was used as carrier, almost no 1-hexene isomers were present in the product. Instead, a large amount of aromatics toluene and xylene were generated, as shown in Table 4. Therefore, we speculate that in olefin aromatization, Ni played a major role in activating olefins into carbocation; then, carbocation followed oligomerization, cyclizing dehydrogenation in the pore of HZSM-5 [29, 32, 33]. On the other hand, nickel also played a key role in desulfurization via removing S atoms from the ring of thiophene. Thus, the high aromatics yield would weaken desulfurization performance because desulfurization and olefin aromatization both require the participation of active Ni sites at the same time.

XRD Results

As shown in Fig. 4, the diffraction peaks at $2\theta = 37.0°$, 43.1°, 62.8°, 74.7°, 78.8° are attributed to NiO (JCPDS-PDF No. 78-0423). The diffraction peaks at $2\theta = 31.7°$, 34.4°, 36.3°, 47.5°, 58.6°, 63.0° belong to ZnO (No. 79-2205). The diffraction peaks at $2\theta = 23.1°$, 23.7°, 24.4° agree with those of HZSM-5 (No. 49-0657). No $NiAl_2O_4$ or $ZnAl_2O_4$ was detected in the adsorbents. The spinel would not generate due to excess Ni or ZnO, and all Ni existed as Ni^{2+} in Ni/ZnO–HZSM-5. As shown in Fig. 5, the regenerated
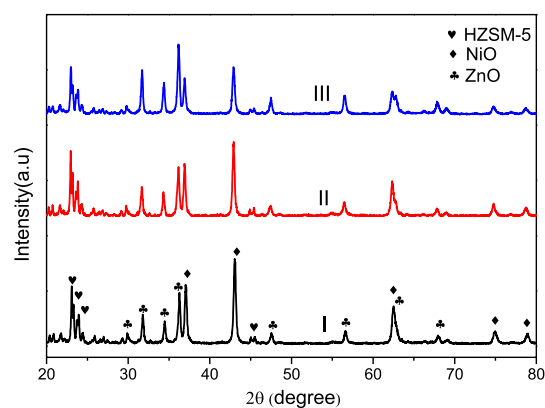

Fig. 4 XRD patterns of Ni/ZnO–HZSM-5-X, X = 1:1 (I), 1:1.5 (II), 1:2 (III)
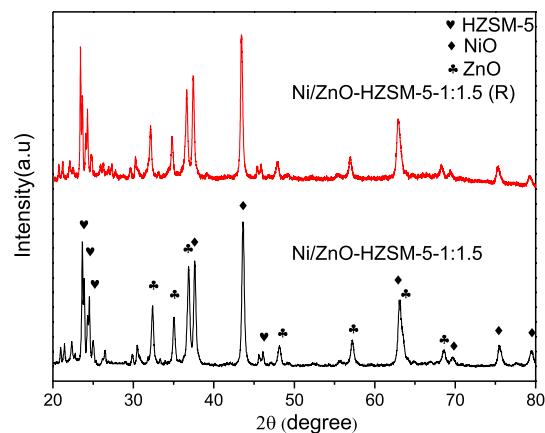

Fig. 5 XRD patterns of fresh and regenerated Ni/ZnO–HZSM-5-1:1.5

adsorbent was compared with the fresh one, and the peak widths and heights were unchanged, suggesting that the

internal structure of regenerated adsorbent has recovered as fresh adsorbents.

H$_2$-TPR Analysis

Ni^0 actively breaks C–S bonds and releases H$_2$S from sulfur-containing compounds. Cleavage of C–S bonds was considered to be the rate-limiting step in RADS [5], which strongly depends upon the reducibility of NiO [18]. Therefore, H$_2$-TPR technique was used to measure the reduction temperature of NiO and to better understand NiO reduction. H$_2$-TPR profile of adsorbent Ni/ZnO–HZSM-5 exhibited one broad H$_2$ consumption peak, as shown in Fig. 6. The intensity of TCD signal presented a positive correlation with Ni content. With higher nickel content, more H$_2$ was consumed by nickel oxide reduction, whereas zinc oxide cannot be reduced without consuming hydrogen in the range of 360–570 °C [34]. The temperature peak of Ni/ZnO–HZSM-5 was the same as that of Ni/ZnO adsorbent, and temperature range of H$_2$ reduction peak also distributed in 360–570 °C, indicating that the NiO sites weakly interacted with HZSM-5 matrix. The temperature peak of the signal appeared at 480 °C, as shown in Fig. 6; the reduction temperature of Ni/ZnO–HZSM-5 was higher than that of pure NiO as the temperature peak of pure NiO is 390 °C [34], suggest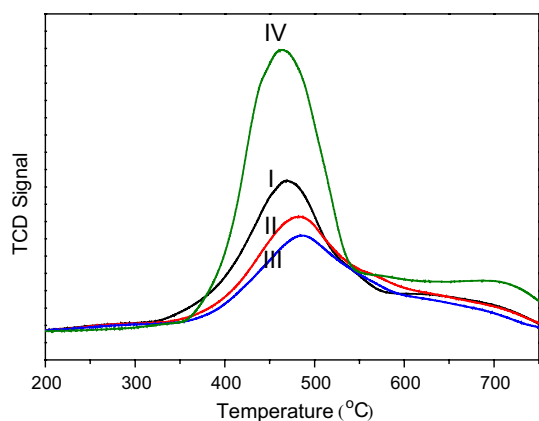ing the strong interaction between NiO and ZnO. Comparing curves I and II in Fig. 6, the temperature peak of signals increased with decreasing Ni to ZnO ratio, suggesting that the intensity of interaction between NiO and ZnO would be reinforced as the content of nickel decreased.

BET Features and NH$_3$-TPD Analysis

Table 5 provides the textural properties and acid amounts of Ni/ZnO–HZSM-5-*X* adsorbents. N$_2$ adsorption/desorption isotherms are typical microporous adsorption belonging to type I isotherms according to IUPAC (Fig. 7a). The PSD of synthetic adsorbents indicated that pore size mainly concentrated at the range of 0.35–0.40 nm, as shown in Fig. 7b. This result suggests that active metal sites caused no damage in the structure of HZSM-5 pore after loading Ni and ZnO compared with the parent HZSM-5. This phenomenon is also consistent with the result of XRD characterization. A more pronounced ascent of the isotherms at high relative pressure ($P/P_0 > 0.9$) was discerned, and this condition was associated with nitrogen adsorption in macropores [35, 36].

Metal oxides changed the acid amount on adsorbent surface, especially the drastic decrease in strong acidity, as shown in Fig. 8. Strong acids play a key role in steps of dehydrocyclization formation of aromatics [37], and strong acid sites are indispensable in olefin aromatization [38]. Song et al. [38] further reported that weak acid sites could catalyze olefin into diolefin or cycloolefin, which are intermediates of olefin aromatization, and strong acids could directly transform mono-olefins into aromatics through hydrogen transfer. Although the strong acid amount of Ni/ZnO–HZSM-5-*X* remarkably reduced, the capacity of catalyzing olefins into aromatics showed no decline. This result implies that Ni or ZnO assists catalysis during the conversion of olefins into aromatics, and condition of decreased strong acid could also efficiently avoid coking and deep cracking resulting from excessive strong acidity [39].

Coke Analysis

The adsorbents were analyzed by TG analysis after reacting for 3 h. Figure 9 shows the TG measurements on used adsorbents and used HZSM-5 under air flow. In addition, hydrogen-reduced fresh Ni/ZnO–HZSM-5-1:2(F) adsorbent

Fig. 6 H$_2$-TPR of Ni/ZnO–HZSM-5-*X* (*X* = 1:1 (I), 1:1.5 (II), 1:2 (III)) and Ni/ZnO-1:1 (IV)

Table 5 Textural properties and acid amounts of adsorbents

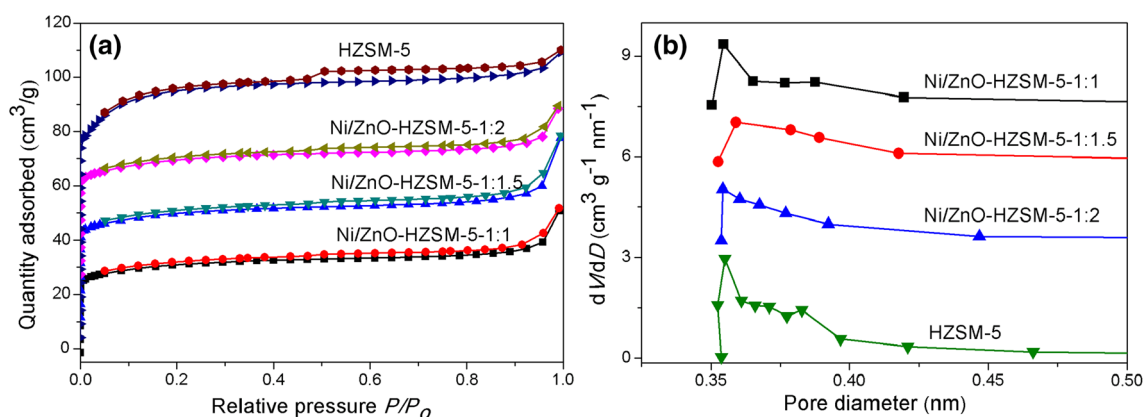| Adsorbent	S_{BET} (m^2/g)	Micropore volume (cm^3/g)	Strong acid amount (mmol/g)	Weak acid amount (mmol/g)	Total acid amount (mmol/g)
HZSM-5	287.1	0.1464	0.235	0.575	0.81
Ni/ZnO-HZSM-5-1:1	131.1	0.06454	0.058	0.479	0.537
Ni/ZnO-HZSM-5-1:1.5	136.8	0.06574	0.021	0.527	0.548
Ni/ZnO-HZSM-5-1:2	146.2	0.07172	0.033	0.433	0.466

Fig. 7 **a** N$_2$ adsorption/desorption isotherms and **b** PSD of Ni/ZnO–HZSM-5-*X* and HZSM-5
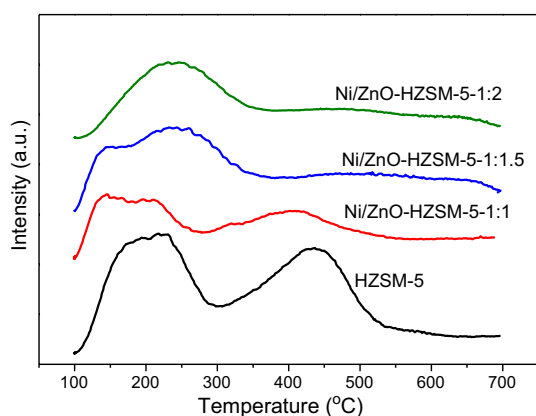

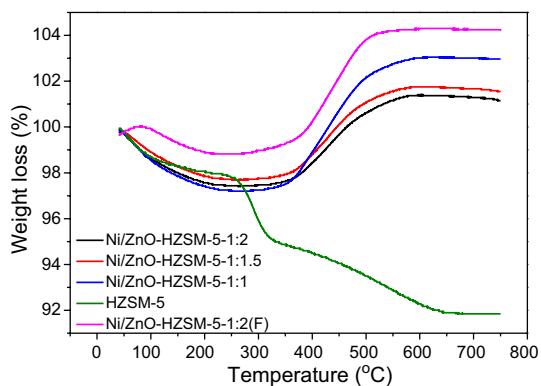**Fig. 8** NH$_3$-TPD profiles of Ni/ZnO–HZSM-5-*X* and HZSM-5

Fig. 9 TG curves of used Ni/ZnO–HZSM-5, used HZSM-5, and hydrogen-reduced fresh Ni/ZnO–HZSM-5-1:2(F) under air flow

was used as a contrast. The curves are divided into two different weight loss stages. The first one can be attributed to the water adsorbed before 250 °C. The second stage between 250 and 650 °C was associated with coke decomposition. However, the weight of used adsorbents rose between 250

and 650 °C. This result was ascribed to the gradual oxidation of Ni in the internal adsorbents into NiO in air flow at high temperature. As for the fresh reduction Ni/ZnO–HZSM-5 (F) adsorbent, the TG curve also rises up and exceeds the initial weight. We can conclude that almost no coke was generated on Ni/ZnO–HZSM-5 adsorbents, and deactivation of adsorbents mainly resulted from sulfur rather than coking. Coking of pure HZSM-5 was more significant than that of Ni/ZnO–HZSM-5. The possible reason is that acid distribution resulted in such situation as strong acids disappeared after HZSM-5 loaded the active metal Ni and ZnO sites, whereas much strong acids distributed on HZSM-5.

Conclusion

The difunctional Ni/ZnO–HZSM-5-*X* adsorbents can achieve deep desulfurization and convert olefins into aromatics at the same time. In olefin aromatization, the active Ni sites cooperated with HZSM-5 to catalyze olefins into aromatics. The Ni/ZnO–HZSM-5-1:1.5 adsorbent could remove 98.0% thiophene with a processing amount 12 mL of model fuel flow, corresponding to the concentration of sulfur under 10 ppm. A competitive relationship exists between thiophene desulfurization and olefin aromatization as these processes require the active Ni sites to participate in reaction at same time. The performance of the different chemical structures in olefin aromatization decreased in the following order: 1-pentene > 2-pentene > 2-methyl-2-butene, and 1-pentene > 1-hexene.

References

1. Wu Y, Wang G, Yang G (2008) Review on the FCC gasoline desulfurization processes. Chem Eng Oil Gas 37(6):499–506 **(in Chinese)**

2. Khare GP (2004) Desulfurization and novel sorbent for same: US 6803343. 2004-10-12

3. Gislason J (2001) Phillips sulfur-removal process nears commercialization. Oil Gas J 99(47):72–76

4. Ju F, Liu C, Meng C et al (2015) Reactive adsorption desulfurization of hydrotreated diesel over a Ni/ZnO–Al$_2$O$_3$–SiO$_2$ adsorbent. Energy Fuels 29(9):6057–6067

5. Huang L, Wang G, Qin Z et al (2010) A sulfur K-edge XANES study on the transfer of sulfur species in the reactive adsorption desulfurization of diesel oil over Ni/ZnO. Catal Commun 11(7):592–596

6. Babich IV, Moulijn JA (2003) Science and technology of novel processes for deep desulfurization of oil refinery streams: a review. Fuel 82(6):607–631

7. Huang L, Wang G, Qin Z et al (2011) In situ XAS study on the mechanism of reactive adsorption desulfurization of oil product over Ni/ZnO. Appl Catal B 106(1–2):26–38

8. Song C (2003) An overview of new approaches to deep desulfurization for ultra-clean gasoline, diesel fuel and jet fuel. Catal Today 86(1):211–263

9. Velu S, Ma X, Song C (2003) Selective adsorption for removing sulfur from jet fuel over zeolite-based adsorbents. Ind Eng Chem Res 42(21):5293–5304

10. Wang G, Wen Y, Fan J et al (2011) Reactive characteristics and adsorption heat of Ni/ZnO–SiO$_2$–Al$_2$O$_3$ adsorbent by reactive adsorption desulfurization. Ind Eng Chem Res 50(22):12449–12459

11. Khare GP (2003) Desulfurization process and novel bimetallic sorbent systems for same: US 6531053. 2003-03-11

12. Khare GP (2007) Sorbent composition, process for producing same and use in desulfurization: EU 1222023. 2007-11-04

13. Wang L, Zhao L, Xu C et al (2016) Screening of active metals for reactive adsorption desulfurization adsorbent using density functional theory. Appl Surf Sci 399(31):440–450

14. Skrzypski J, Bezverkhyy I, Safonova O et al (2011) 2.8Ni–H$_{1.8}$Ni$_{0.6}$(OH)MoO$_4$—Novel nanocomposite material for the reactive adsorption of sulfur-containing molecules at moderate temperature. Appl Catal B Environ 106(3):460–468

15. Ju F, Liu C, Li K et al (2016) Reactive adsorption desulfurization of fluidized catalytically cracked (FCC) gasoline over a Ca-doped Ni–ZnO/Al$_2$O$_3$–SiO$_2$ adsorbent. Energy Fuels 30(8):6688–6697

16. Yu F, Yin J, Gang S et al (2009) Mechanistic pathways for olefin hydroisomerization and aromatization in fluid catalytic cracking gasoline hydro-upgrading. Energy Fuels 23(6):3016–3023

17. Qiu L, Zou K, Xu G (2013) Investigation on the sulfur state and phase transformation of spent and regenerated S zorb sorbents using XPS and XRD. Appl Surf Sci 266(2):230–234

18. Ullah R, Bai P, Wu P et al (2017) Cation–anion double hydrolysis derived mesoporous mixed oxides for reactive adsorption desulfurization. Microporous Mesoporous Mater 238:36–45

19. Tsybulevski AM, Tkachenko OP, Rode EJ et al (2017) Reactive adsorption of sulfur compounds on transition metal polycation-exchanged zeolites for desulfurization of hydrocarbon streams. Energy Technol 5(9):1627–1637

20. Wei Z, Chen L, Cao Q et al (2017) Steamed Zn/ZSM-5 catalysts for improved methanol aromatization with high stability. Fuel Process Technol 162:66–77

21. Li Y, Liu S, Zhang Z et al (2008) Aromatization and isomerization of 1-hexene over alkali-treated HZSM-5 zeolites: improved reaction stability. Appl Catal A 338(1):100–113

22. Ma D, Lu Y, Su LL et al (2002) Remarkable improvement on the methane aromatization reaction: a highly selective and coking-resistant catalyst. J Phys Chem B 106(34):8524–8530

23. Yin C, Zhao R, Liu C (2005) Transformation of olefin over Ni/HZSM-5 catalyst. Fuel 84(6):701–706

24. Min YG, Song C, Kim TH et al (2017) BTX production by coaromatization of methane and propane over gallium oxide supported on mesoporous HZSM-5. Mol Catal 439:134–142

25. Tamiyakul S, Sooknoi T, Lobban LL et al (2016) Generation of reductive Zn species over Zn/HZSM-5 catalysts for n-pentane aromatization. Appl Catal A 525:190–196

26. Su X, Zan W, Bai X et al (2017) Synthesis of microscale and nanoscale ZSM-5 zeolites: effect of particle size and acidity of Zn modified ZSM-5 zeolites on aromatization performance. Catal Sci Technol 7(9):1943–1952

27. Janjic N, Scurrell MS (2002) Evidence for the enhancement of the catalytic action of Zn-ZSM-5-based catalysts for propane aromatization using microwave radiation. Catal Commun 3(6):253–256

28. Chen Z, Xu J, Yu F et al (2015) Reaction mechanism and kinetic modeling of hydroisomerization and hydroaromatization of fluid catalytic cracking naphtha. Fuel Process Technol 130:117–126

29. Vedrine JC, Dejaifve P, Garbowski ED et al (1980) Aromatics formation from methanol and light olefins conversions on H-ZSM-5 zeolite mechanism and intermediate species. Stud Surf Sci Catal 5:29–37

30. Zheng XC, Ponec V (1994) On the problems of the mechanism of the skeletal isomerization of n-butene. Catal Lett 27(1–2):113–117

31. Houzvicka J, Ponec V (1997) Skeletal isomerization of butene: on the role of the bimolecular mechanism. Ind Eng Chem Res 36(5):1424–1430

32. Lukyanov DB, Gnep NS, Guisnet MR (1994) Kinetic modeling of ethene and propene aromatization over HZSM-5 and Ga-HZSM-5. Ind Eng Chem Res 33(2):223–234

33. Lukyanov DB (1997) Application of a kinetic model for investigation of aromatization reactions of light paraffins and olefins over HZSM-5. Stud Surf Sci Catal 105:1301–1308

34. Tang M, Zhou L, Du M et al (2015) A novel reactive adsorption desulfurization Ni/MnO adsorbent and its hydrodesulfurization ability compared with Ni/ZnO. Catal Commun 61:37–40

35. Qin Z, Lakiss L, Gilson JP et al (2012) Chemical equilibrium controlled etching of MFI-type zeolite and its influence on zeolite structure, acidity, and catalytic activity. Chem Mater 25(14):2759–2766

36. Dai C, Zhang A, Li L et al (2013) Synthesis of hollow nanocubes and macroporous monoliths of silicalite-1 by alkaline treatment. Chem Mater 25(21):4197–4205

37. Lucas AD, Canizares P, Duran A et al (1997) Coke formation, location, nature and regeneration on dealuminated HZSM-5 type zeolites. Appl Catal A 156(2):299–317

38. Song Y, Zhu X, Xie S et al (2004) The effect of acidity on olefin aromatization over potassium modified ZSM-5 catalysts. Catal Lett 97(1–2):31–36

39. Lin X, Yu F, Liu Z et al (2007) A novel method for enhancing on-stream stability of fluid catalytic cracking (FCC) gasoline hydro-upgrading catalyst: post-treatment of HZSM-5 zeolite by combined steaming and citric acid leaching. Catal Today 125(3–4):185–191